Defence Research and Development Canada | Recherche et développement pour la défense Canada

CAN UNCLASSIFIED

DRDC | RDDC
technologysciencetechnologie

Exploring Terahertz Waves for Submarine Cladding Non-Destructive Examination (NDE)

Tile Sealant Transmission Characterization, Instrument Field Housing Design/Prototype Option B: proof-of-concept concealed interface imaging

Matt Reid
Patrick Kilcullen
UNBC

Prepared by:
University of Northern BC
3333 University Way
Prince George, (BC) V2N 4Z9
Canada
Client Ref. No.: W7707-16-5881
PSPC Contract Number: W7707-155881/001/HAL
Technical Authority: Rod McGregor, Defence Scientist
Contractor's date of publication: March 2017

Defence Research and Development Canada

Contract Report
DRDC-RDDC-2018-C200
February 2019

CAN UNCLASSIFIED

Canada

Final Report: March 21, 2017
Prepared by: Matt Reid

Title: Exploring Terahertz Waves for Submarine Cladding NDE: Tile Sealant Transmission Characterization, Instrument Field Housing Design/Prototype Option B: proof-of-concept concealed interface imaging

List of contributors

University of Northern BC
Matt Reid
Patrick Kilcullen

Subctontract:
Spectrum NDT
Jordan Hynes
Brian Gray

DRDC Research Liaison: Rod McGregor

Executive summary: A Brewster angle imaging system was developed for subsurface hull inspection using broad-band pulsed THz radiation using a Picometrix T-Ray 4000 system in a previous phase of this project. Additionally, a single frequency, reflection imaging prototype system was developed using a cw TeraSense sub-THz imaging camera for subsurface interface inspection. Both systems were previously used to look at the possibility of a submarine hull inspection application for water ingress below Sikaflex grout lines, as it was identified that the grout-lines held the only potential for though-cladding hull inspection in the far-infrared. Additionally, the possibility of using microwave frequencies was studied by subcontracting microwave inspection to Spectrum NDT. It was identified that through-Sikaflex inspection was not possible at frequencies of potential transparency at frequencies in the far-infrared and below (below 2 THz). In order to generally explore the suitability for subsurface interface water ingress detection of the developed prototypes at all frequencies, the project was extended as per Option B, to demonstrate the potential of the envisioned systems to tackle the identified problem using an analogue sample as the cladding, to demonstrate the idea. As such, this report summarizes the potential for the envisioned application in the far infrared using (i) the pulsed THz Brewster angle imaging system developed in the previous phase, (ii) the cw TeraSense reflection imaging system prototype developed in the previous phase, and (iii) the evisive scan microwave system subcontracted in the previous phase of this project. The results demonstrate the proof-of-principle of concealed interface inspection is possible, and we offer insight into subsurface interface inspection and moisture detection at frequencies from microwave to THz.

Table of Contents

1.0 – THz radiation evaluation: Spectroscopy was performed in transmission through 1" thick analogue tiles previously studied (sample A1-6), and new 1" thick sample coverings to compare the THz transmission properties. All measurements were conducted on-site, and it was determined that the samples were substantially more transparent than the analogue tiles, allowing us to explore the proof-of-concept reflection imaging which is described in subsequent sections. All spectroscopic measurements were made with the Picometrix THz time-domain spectroscopy system in a simple transmission geometry (pitch-catch transmitter-receiver geometry with the samples in the middle).

1.1 - THz time-domain signals. The reference THz signal (through air) is shown in Fig. 1.1.1 below (black). The signal through the sample (red) and analogue tile (A1-6, blue) is also shown for comparison. The field amplitude transmitted through 1" of the sample is approximately 5x larger than what is transmitted through the analogue tiles, which translates to 25x more power, indicating significantly more transmission. The result is that the sample material is appropriate for studying proof-of-concept concealed subsurface reflection imaging. The spectroscopic properties are shown in the next section.

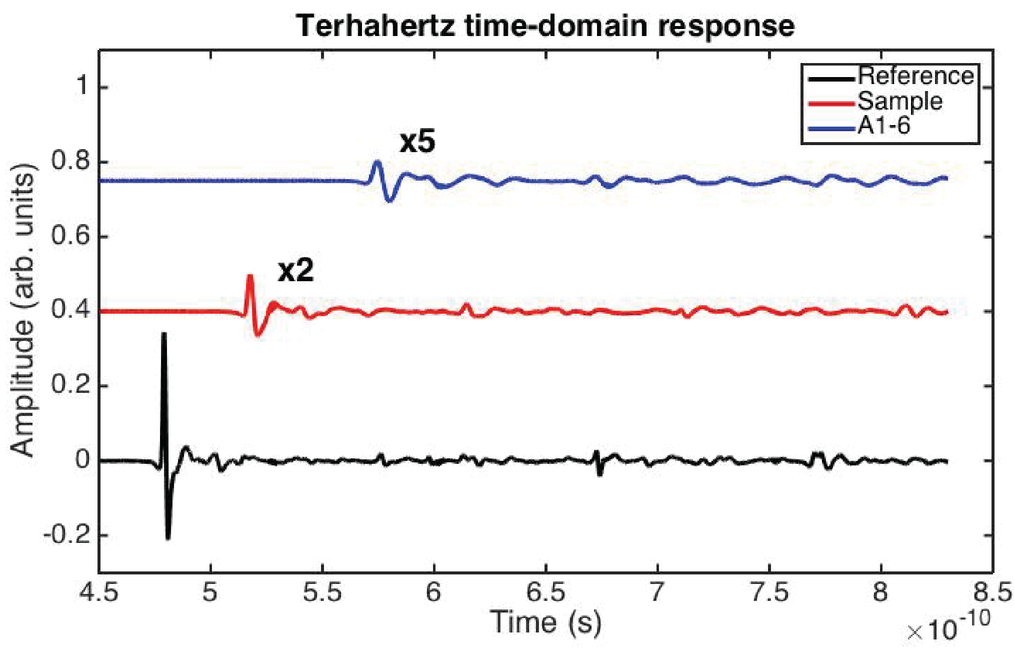

Fig. 1.1.1 – THz time-domain signal response through 1" of analogue tile (A1-6, blue) and sample covering material (red), scaled by 5x and 2x respectively. Reference (through air) is shown in black for comparison.

1.2 - THz sample spectroscopy. Spectroscopy was conducted by using the data of Fig. 1.1 to determine the absorption coefficient (Fig. 1.2.1) and index of refraction (Fig. 1.2.2) of both the analogue tiles previously studied, and the new sample covering material.

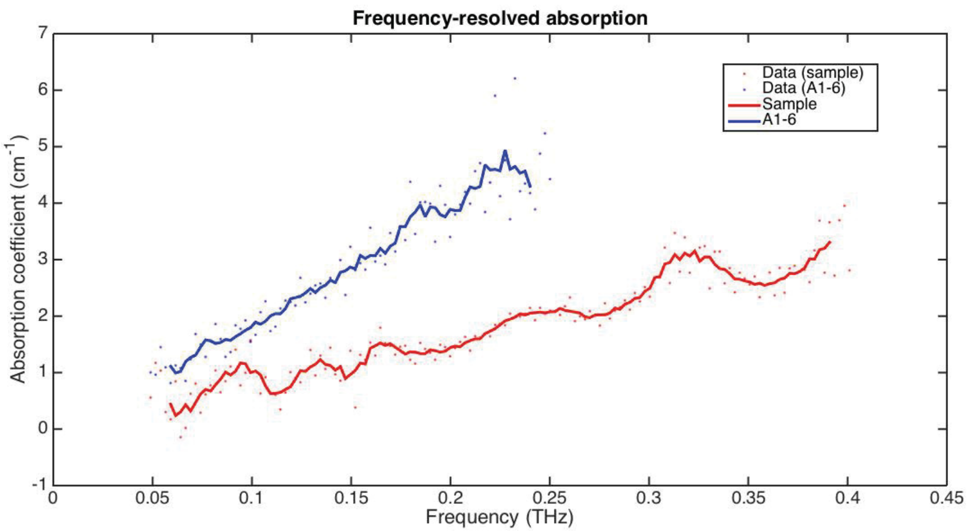

Fig. 1.2.1 – Absorption coefficient of 1” thick analogue tile (A1-6, blue) and 1” thick sample covering (red). The dots are measured data points calculated from Fig. 1.1.1, and the solid curves are the curves smoothed using a 5-point moving average. The calculation is performed in an identical manner to the previous phases of this project.

The sample covering (red) in Fig. 1.2.1 extends to a higher frequency (~400 GHz) than the analogue tile material (250 GHz) because of the smaller absorption (noticeable also in Fig. 1.2.2 below, and Fig. 1.1.1). The absorption coefficient is only about 1 cm^{-1} at 200 GHz in comparison to 3 cm^{-1} for the analogue tiles used previously.

In addition to a lower absorption coefficient, the sample covering shows a significantly lower index of refraction (1.4 vs. 2.1) in comparison to A1-6. While this is good from a loss perspective for concealed interface imaging, it means that the Brewster angle is different than what was designed for the analogue tiles. This is discussed further later in the report.

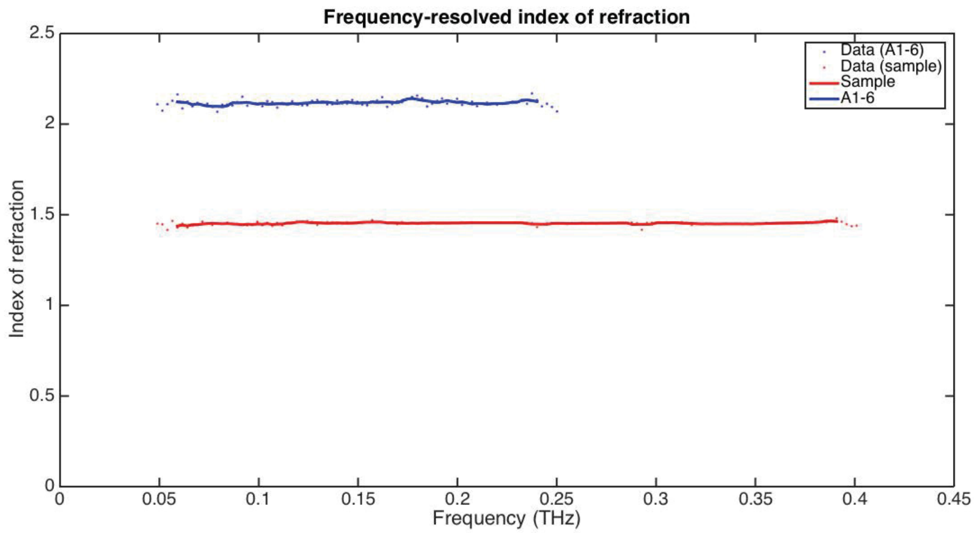

Fig. 1.2.2 – Index of refraction of 1" thick analogue tile (A1-6, blue) and 1" thick sample covering (red). The dots are measured data points calculated from Fig. 1.1.1, and the solid curves are the curves smoothed using a 5-point moving average. The calculation is performed in an identical manner to the previous phases of this project.

Based on these frequency-resolved measurements, it is clear that the sample coverings are much more transparent than the analogue tiles previously studied, especially at 100 GHz (the frequency of the prototype scanning system) and lower (appropriate for the microwave scanning). We therefore conclude that the covering is appropriate to the st the proof-of-concept for measurement of concealed interfaces and interfacial water.

<u>2.0 – Terahertz systems used for measurements.</u>

<u>2.1 – Pulsed THz Brewster Angle Imaging System</u>. This system is identical to what was designed and used in the first phase of this project for measurements with the analogue tiles (please refer to report "Terahertz radiation for Submarine Hull Inspection Through Acoustic Tiles: Evaluation of imagery and spectroscopy effectiveness across a spectrum of incident energies and wavelengths using laboratory and portable COTS systems"). The set-up is shown below in Fig. 2.1.1.

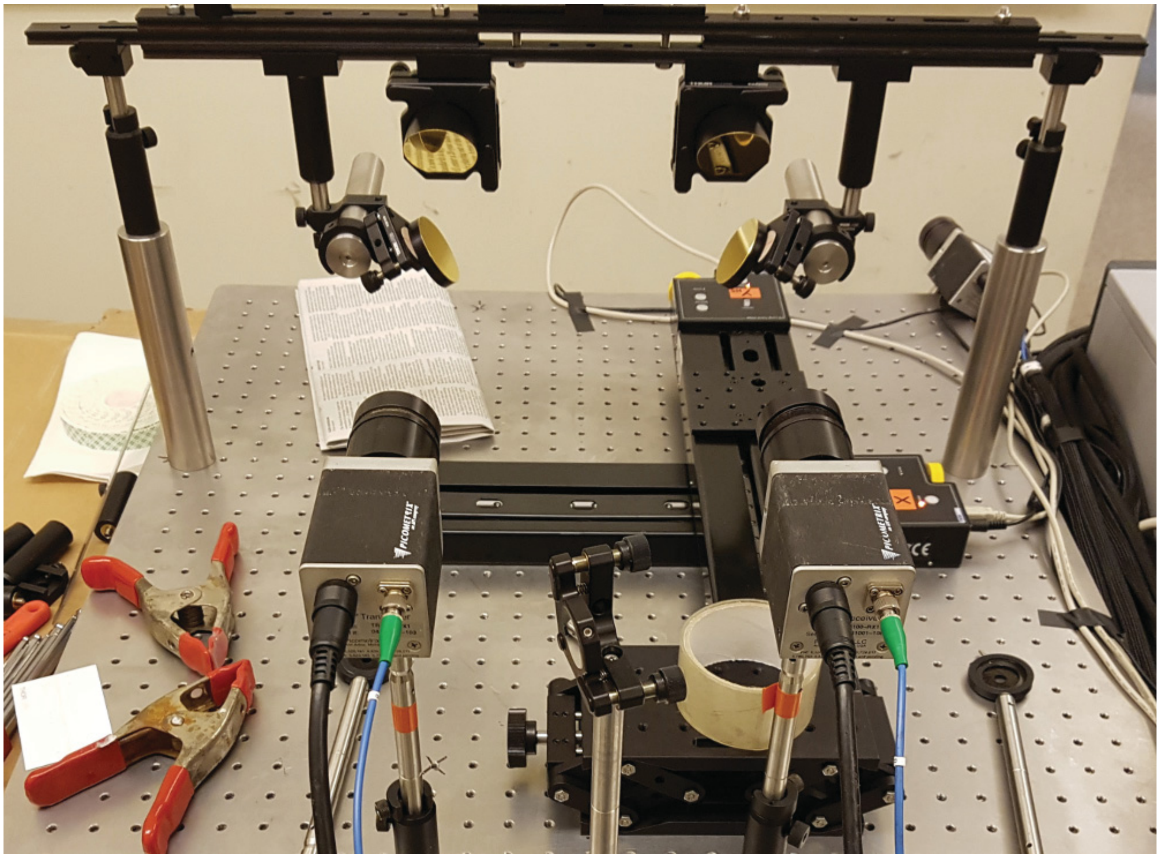

Fig. 2.1.1 – Brewster angle imaging system deployed on-site in this phase of the project.

The figure (Fig. 2.1.1) shows the Brewster angle set-up, whereby the radiation from the transmitter (left, bottom) is collected by the first parabolic mirror (left, top) and focused onto the sample of study using a mirror (left, top) to direct the THz beam onto the sample at an angle of incidence equal to approximately 60^{o}. The radiation is collected in the reflection geometry using a flat mirror (right, top) and parabolic mirror (right, top) to collect the radiation onto the detector (right, bottom). The test plate is mounted with the sample covering on the x-y translation stage which is raster scanned to form an image. It should be noted that this configuration was identified in a previous phase of the project, and the Brewster angle is not optimal for the new index of refraction of the covering sample which is lower than that of the analogue tile the system was designed for (see Fig. 1.2.1). Specifically, Brewster's angle for the analogue tile (n=2.1) is 64^{o}, where it is only 54^{o} for the sample covering (n=1.4). While not optimally oriented for the Brewster angle, clear results could still be obtained. The system was aligned so as to be sensitive to the concealed front surface of the test plate.

2.2 - cw TeraSense Reflection Imaging Prototype. This is the first deployment of the prototype system developed in the previous phase of this project. It is intended to operate as follows.

- Reflection mode imaging for subsurface inspection
- Minimizing front-surface reflections that can obscure concealed interface back-reflections
- Maximizing contrast for subsurface interface imaging

The operation is similar to the Brewster angle reflection imaging system based on the Picometrix system described above. In order to minimize front-surface reflections, linearly polarized light is used at Brewster's angle. For the THz radiation incident from air (n_o = 1.0) into a dielectric material of index n, the angle of incidence is fixed to $\theta_B = tan^{-1}(n)$. The angle depends on the material, but for most that do not absorb strongly, a precise angle is not necessary. Nonetheless, for the specific angle, the THz radiation will be refracted at the front surface of the sample under study, reflected from the subsurface interface, and refracted back out to the detector (refer to the geometry in Fig. 2.2.1 below). This leads to a difference, Δz, in position of the geometrical focal point, and the actual point of reflection at the subsurface. The offset is calculated for a particular angle/material, in order to get proper alignment. Once the geometry is fixed for a particular material of fixed thickness, it can be scanned across that sample to image the concealed interface. The principle is shown in the schematic diagram of the system below.

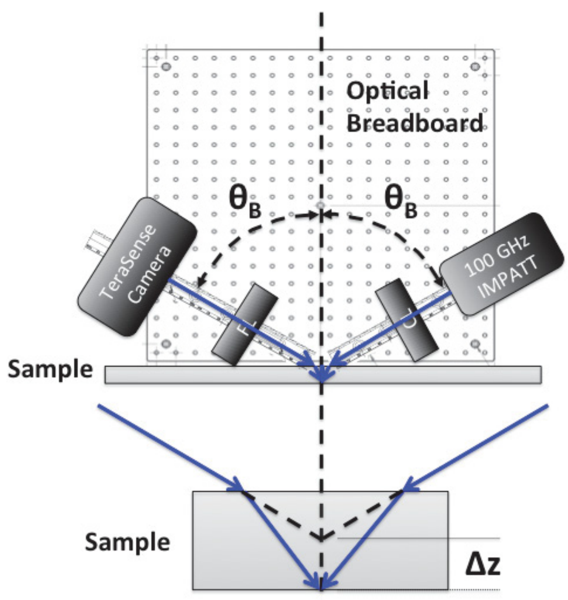

Fig. 2.2.1 – Prototype reflection scanning system design. The source and camera are mounted so as to be at Brewster's angle. The offset resulting from refraction at the sample surface, which depends on sample thickness, is calculated to fix the source-camera geometry.

The TeraSense camera is sensitive to vertical polarization, and so is rotated to be sensitive to horizontal polarization. Similarly, the vertically polarized IMPATT diode is mounted such that the polarization is horizontal (in the plane of the optical breadboard), so that it is p-polarized to be able to achieve Brewster's angle. The camera and source are mounted on optical rails so that their positions can be adjusted relative to two lenses, a collimating lens for the THz source, and a focusing lens to the camera. The relative positions of lens/camera and lens/source are adjusted to achieve the strongest signal on the camera. Both lenses are Teflon lenses with 10 cm focal lengths. A second optical breadboard covers the entire system, and the whole thing can slide across the surface of a sample to be inspected.

The prototype can be operated with real-time readout using a USB connection to the camera and the manufacturer's software. We developed a Matlab library of routines that allows importing data directly from the camera into Matlab. The system is enclosed between two metal plates with wheels mounted for ease of scanning. The full prototype is shown below in Fig. 2.2.2.

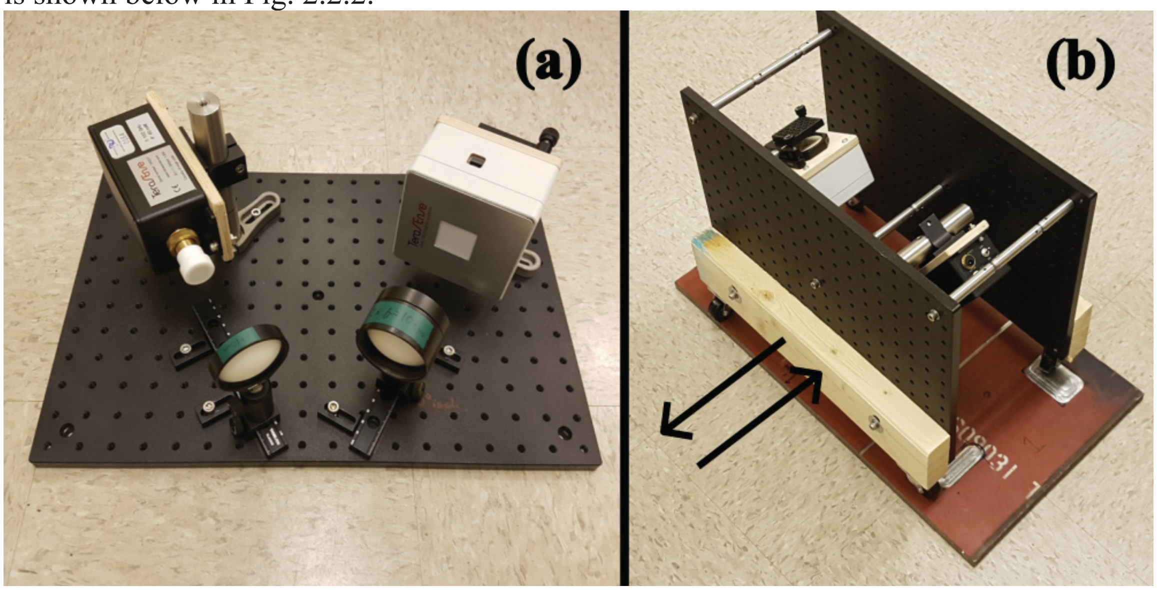

Fig. 2.2.2 – Prototype reflection scanning system layout (a) and implementation (b). The source and camera are mounted so as to be at Brewster's angle. The offset resulting from refraction at the sample surface, which depends on sample thickness, is calculated to fix the source-camera geometry. The system is shown on wheels for easy placement over the test plate shown under the scanner in (b).

<u>*2.3 - Microwave sensing using Evisive scan.*</u> Spectrum NDT was contracted to make complementary microwave measurements on the test panel. The primary sensor head used operated at 24 GHz, with a wavelength of 1.25 cm, and an additional sensor head operating at 10 GHz was also used. The microwave equipment that was used is a first-gen portable hand scanner. It uses an infrared camera and a tracker on the probe to follow the location of the probe and map the distance traveled. The operator must physically

move to probe back and forth so there can be non-relevant indications from probe wobble on the images. The full report from Spectrum NDT is provided in Appendix 1.

<u>3.0 – Test plate scanning.</u> DRDC prepared a test panel for proof-of-concept measurements. The test plate drawing schematic is shown below in Fig. 3.0.1, with an optical image in Fig. 3.0.2 prior to covering with 1” thick sample to conceal the test plate surface. It contains rectangular geometries milled into the surface a few mm deep, with one having a hole milled in the center a few more millimeters deep. For testing, the cavities were imaged while they were filled with water and air in order to see the specificity to interface material, as well as wet spots introduced on the bare metal to check for sensitivity to the presence of interfacial water.

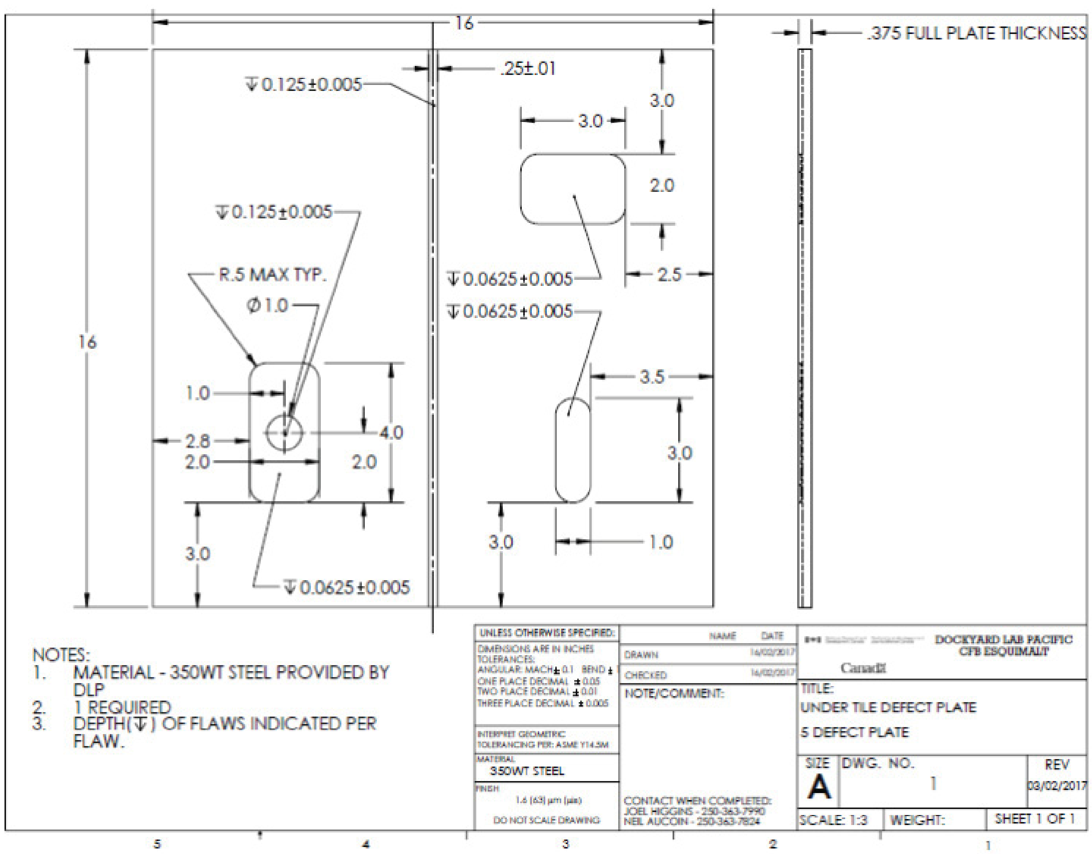

Fig. 3.0.1 – Machine drawing of test panel prepared by DRDC for proof-of-concept concealed interface scanning.

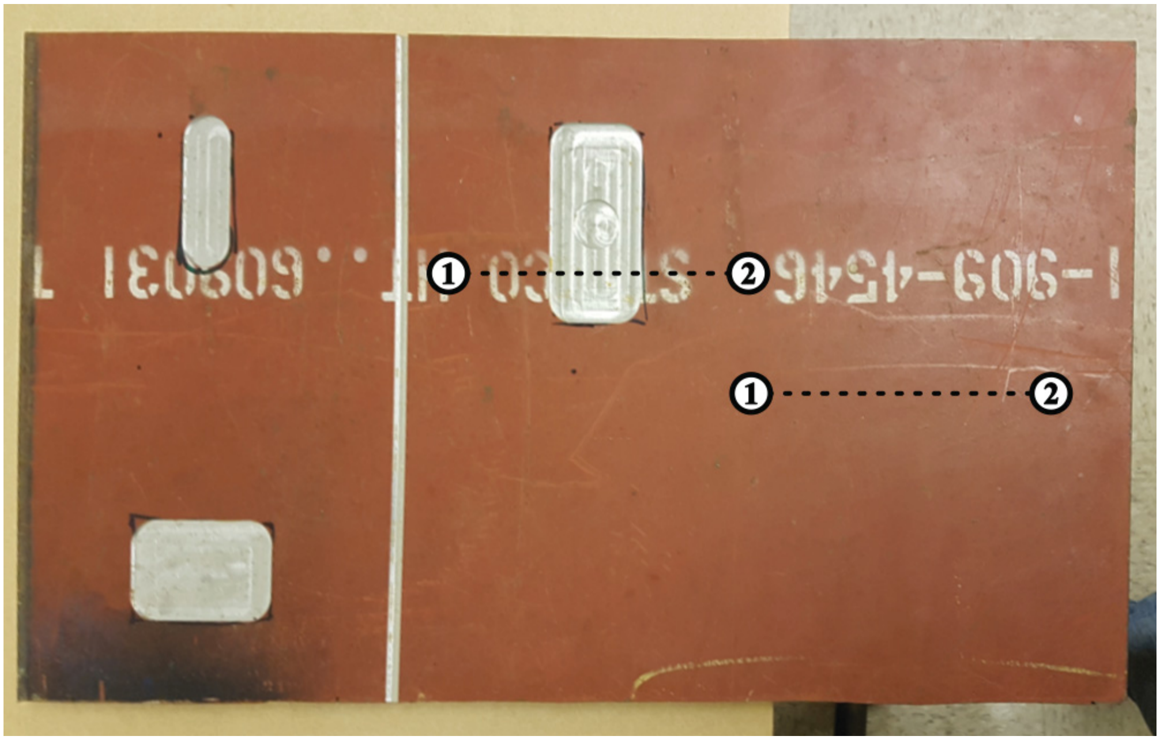

Fig. 3.0.2 – Test panel prepared by DRDC and provided to UNBC (prior to filling voids with water and covered with sample to conceal the test panel surface). The region marked with dashed lines is the region across which the cw prototype system was scanned, as will be discussed later in this section.

<u>3.1 – Broadband, pulsed THz imaging of test plate with sample covering.</u> The sample material, 1” thick, was placed on top of the test plate and put into the pulsed THz Brewster angle imaging system (see Fig. 2.1.1). The sample material is visibly opaque, and so the test is looking at the ability of the THz imaging system to make images of the concealed interface of the test plate shown in Figures 3.0.1 and 3.0.2. Specifically, we focused on the region containing the rectangle with the hole in the middle (right of Fig. 3.0.2). The milled out rectangular region was imaged with water in the cavity. Unfortunately, the water was drawn out of the cavity and into the interface between covering and plate. However, this was fortuitous in the sense that it became apparent that the imaging system could detect the very thin layer of water that was drawn into the interface (see Fig. 3.1.1)

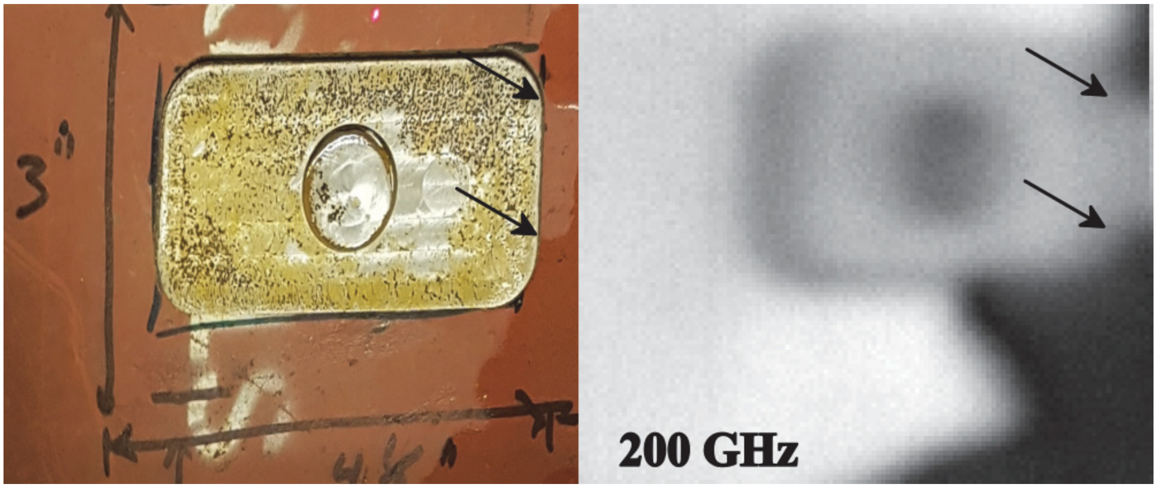

Fig. 3.1.1 – Test panel (left) imaged using the 200 GHz spectral component of the pulsed THz subsurface imaging (right). The arrows show noticeable correlation between the optical picture of the water ingress (left) and the dark region corresponding to THz sensed water ingress (right).

We believe the thin layer of water is what is being picked up in the image on the right at 200 GHz in Fig. 3.1.1. Interestingly, we have access to a variety of wavelengths to make these images with the broadband Picometrix system, and doing so produces the results shown in Fig. 3.1.2 below.

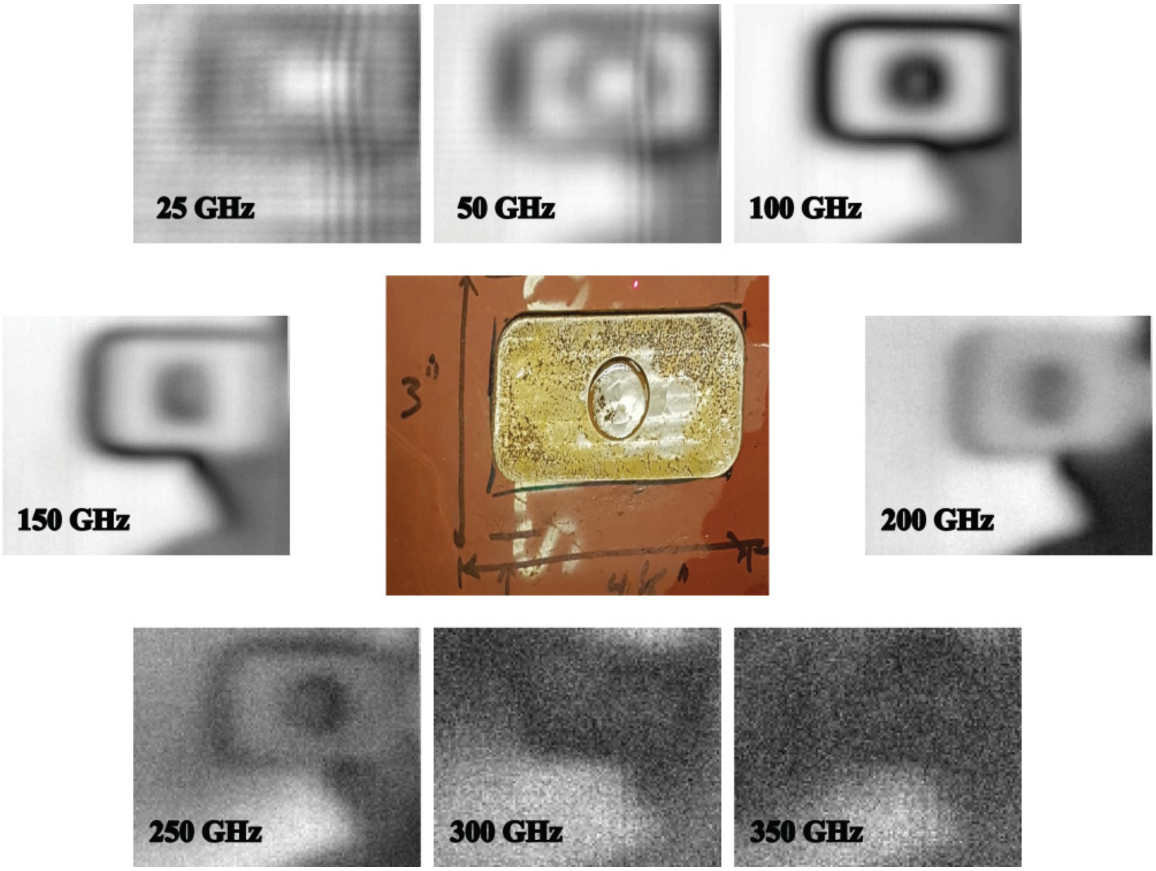

Fig. 3.1.2 – Test panel (center) imaged using the different frequencies available (labeled).

What is clear from Fig. 3.1.2 is that if the dark region in the 200 GHz image is indeed water ingress between the covering and plate, then the response has a greatest contrast at this frequency. In particular, as the frequency increases from 25 GHz, the contrast of the water improves to 200 GHz (while the resolution and fringing from edges reduces). Beyond this frequency, the contrast would appear to decrease, which is likely a result of the reduced signal and increased noise at the higher frequencies. Nonetheless, it would appear that water is visible at 100GHz, but the visibility decreases as the frequency is lowered, which we will revisit in the next section.

In order to test the hypothesis that the water is detectable and that water films are what are being detected in Fig. 3.1.1 and 3.1.2, we conducted a quick scan (coarse resolution) of the same rectangular region, but placing water in the middle circle. The water was placed, and held by its surface tension, to make contact with the sample covering (as verified by it being wet only over the are of the circle upon removal), and not extending into the larger rectangular region. The result is compared directly against the same conditions without the water, and shown in Fig. 3.1.3 below.

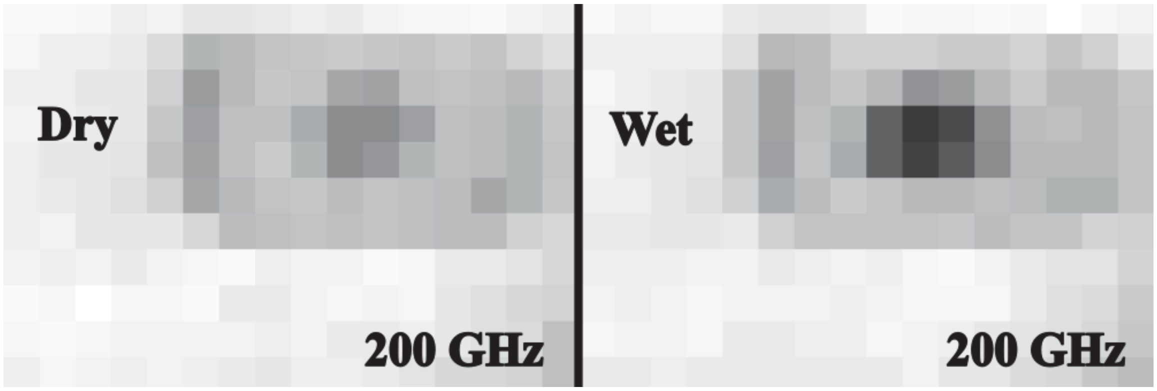

Fig. 3.1.3 – Test panel (rectangular region with hole) imaged at 200 GHz on a coarse scale with only air concealed (left) and with water in the center, air in the remaining portion of the rectangle (right).

The results shown in Fig. 3.1.3 strongly suggests a measurable difference between only air in the void (left), and air with water in the center (right). A higher resolution image with water only in the central circular void is shown in Fig. 3.1.4 below, consistent with the coarse image in Fig. 3.1.3.

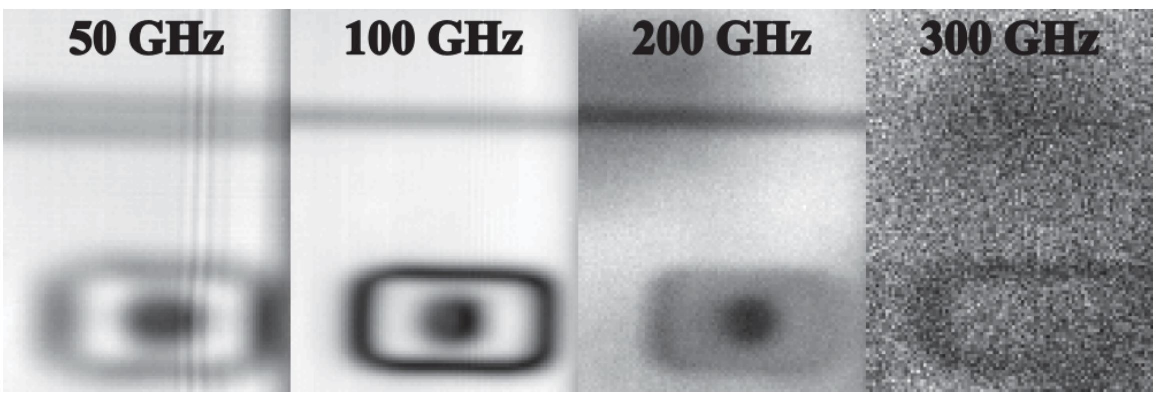

Fig. 3.1.2 – Test panel (rectangular region with hole) imaged at different frequencies on a fine scale with water in the center circular hole, air in the remaining portion of the rectangle (right).

If this is compared to the high resolution image where the water was pulled into the interface, it is clearly seen that the center appears differently when it is filled with water (dark, Fig. 3.1.4) in comparison to when it is filled with air (light, Fig. 3.1.1)

This suggests that the interpretation of sensitivity to interfacial water is what is being identified in the images. In order to definitively answer the question, we conducted a test where a small amount of water (a few drops or ml) was placed at the interface of the metal, and an image produced as shown in Fig. 3.1.4. Note that the metallic region in the absence of interfacial water appears very uniform in 3.1.3, and so deviations from uniformity should indicate the presence of water.

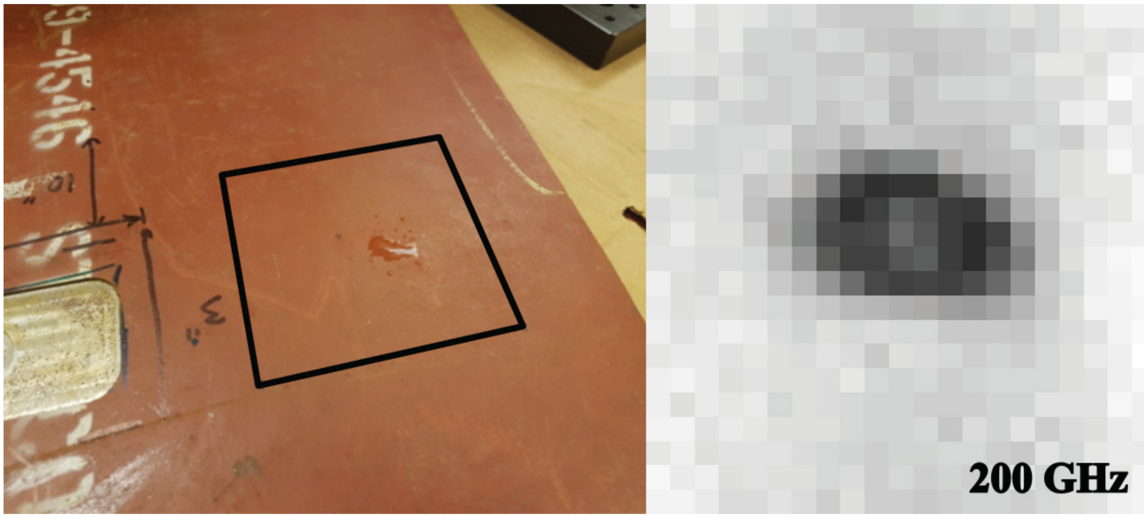

Fig. 3.1.4 – Test panel (left) imaged at 200 GHz (right) on a coarse scale. Notice the water in the optical image (black square on left) correlates with dark spot in THz image (right).

Several tests to image the wet spot were conducted, and we are quite confident that indeed, the 200 GHz images are very sensitive to interfacial water, consistent with the interpretation of the images presented here.

3.2 - Microwave imaging of test plate with sample covering using Evisive Scan. Similar tests to those conducted above were carried out using the Evisive Scan microwave system operated by Spectrum NDT. The full report is provided in Appendix 1. The conclusions that were obtained with respect to the microwave interferometric measurement of the concealed interface were as follows:

- The machined areas (i.e. larger air gaps) were quite easy to locate, and their varying depths have an influence on signal return
- The presence of water can alter the signal return notably
- The sample covering (as inspected) is transparent to microwave energy at 10 – 25 GHz

The water is reflecting a signal to a certain extent, however it is unknown how much water is required to create the signal difference. As well, it is unknown whether the water is creating the signal change, or if the water is indeed creating a changing air gap between the panel and the steel backing.

Based on the results of the experiment it can be concluded that microwave energy can be used to see through a dielectric material and differentiate properties of the interface and conductive backing material.

3.3 - cw THz imaging of test plated with covering using prototype system. Single-frequency reflection imaging was attempted at 102 GHz using the 60 mW cw source and sub-THz imaging camera incorporated into the prototype system described in section 2.2. The imaging camera had a resolution of 16 by 16 pixels with an approximate pixel pitch of 1.2 mm. In contrast to the Picometrix time-domain imaging system, the TeraSense equipment operates at a single wavelength and only records intensity information. The radiation output from the source was linearly polarized, and was aligned in reflection with the preferred polarization direction of the camera.

In order to distinguish signals reflected from the front and back metal surfaces, reflecíton imaging was attempted for TM polarized radiation at a 30^o angle of incidence in order to allow for a geometrical offset between the front and back surface reflected rays. The setup featured two sets of millimeter wave lens assemblies to both collimate the source beam and image the back surface onto the camera. The plane of the sub-THz source and camera was then mounted vertically onto a rolling chassis. The height of the chassis was chosen in order to align the back surface reflected signal with the optical axis of the camera.

Live camera output was then viewed for a specific group of pixels near the far top extent of the camera which corresponded to the pixels furthest form the large front surface reflection. The camera output from these pixels was summed and plotted as the apparatus was rolled across the top surface of the sample placed on top of a metal backing plate.

Unfortunately, imaging results with the attempted apparatus were not conclusive. As illustrated by the rolling line scans shown in Fig. 3.3.1, intensity scans taken across the sample when backed by contiguous metal (a) were dominated by changes in the front surface reflection as the chassis was moved. Although the intensity scan taken across the milled slot (b) showed multiple peaks, the magnitude of the variations in comparison with (a) suggest that these peaks may be due to the front surface reflection.

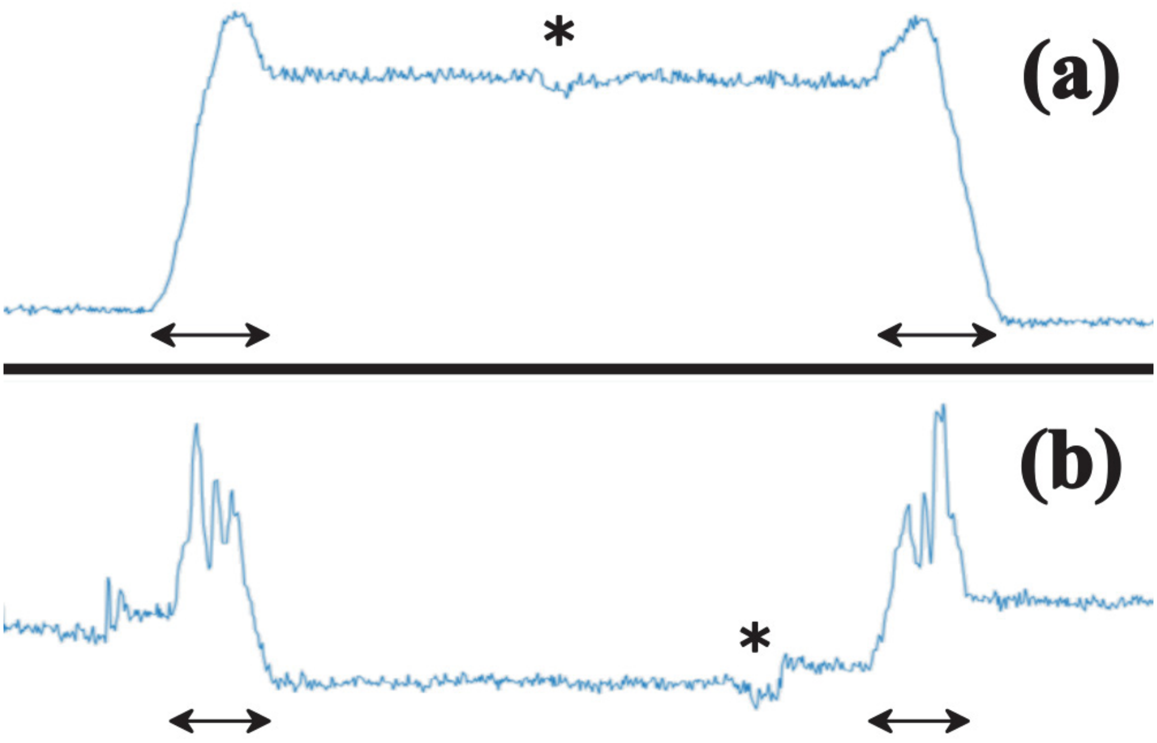

Fig. 3.3.1 – Live camera output (left to right) from the two line scans shown in the metal plate figure (Fig. 3.0.2). (a) Contiguous metal line scan. The two underset arrows locate the movement of the rolling cart from location (1) to (2), and then from location (2) to (1) (as shown on Fig. 3.0.2). (b) Line scan taken over the milled slot. The underset arrows again indicate chassis movement from (1) to (2), and then from location (2) to (1). The asterisk symbol (*) indicates small disruptions caused by a re-alignment of the rolling wheels of the apparatus.

While this preliminary scan using the prototype did not reveal the underlying structure to our satisfaction, sample transparency and successful imaging at 100 GHz was demonstrated with the Picometrix imaging setup. This suggests that if successful measures to eliminate the front surface reflection are implemented, detections of back surface reflected signals with the TeraSense setup could be possible. Such future measures for front surface signal blocking could include operating closer to the Brewster angle (which was different for this case than with the Analogue tiles considered previously), as well as additional shields to narrow and collimate the sub-THz source.

It should also be noted that another source of error may have been the dynamic range of the configuration. In order for the front surface reflection not to saturate the camera, the intensity scale was adjusted for the front surface reflection intensity which was not minimized by appropriately being at Brewster's angle because of the difference in index of refraof refraction between the sample covering used here and the original analogue tiles (A-6, eg) as shown in Fig. 1.1.2. As such, the interface reflection may simply have been below the noise floor in this configuration, but could easily be increased through increasing the integration time.

In summary, while the prototype did not yield definitive results, there is reason to believe it could be useful for the target application based on the pulsed THz images obtained, but more work is required to prove this.

4.0 – Recommendations for future work. While the conclusions from this work have been stated throughout, I summarize the results and recommendations concisely in this section.

4.1 – Summary of observations. We observed the following

- Test plate sample coverings (~1" thick) were used with significantly reduced absorption in comparison to previous analogue tiles, and therefore higher transparency to prove the principle of subsurface interface imaging (at frequencies from microwave into the THz range).
- Pulsed THz imaging of concealed interfaces is possible, with good spatial resolution, and able to detect air voids easily at frequencies from about 50 GHz – 300 GHz.
- Pulsed THz imaging of concealed interfacial water is possible, even with thin layers of moisture resulting from water ingress
- It seems 200 GHz is about the optimal wavelength for interfacial water sensitivity
- Subsurface interface imaging with the prototype TeraSense scanner yielded inconclusive results.
- 100 GHz - corresponding to the single wavelength TeraSense frequency - is adequate to reveal water (although that system yielded inconclusive results in this test).
- 200 GHz single frequency units are also available from TeraSense.
- Concealed interface microwave imaging was demonstrated with the Evisive Scan system.
- The machined areas (i.e. larger air gaps) were quite easy to locate, and their varying depths have an influence on signal return from the microwave system (10-25 GHz)
- The presence of water can alter the microwave signal return notably
- The sample covering (as inspected) is transparent to microwave energy at 10 – 25 GHz

4.2 – Recommendations. We make the following recommendations

- Further work with the prototype TeraSense system is justifiable given both microwave and higher frequency THz concealed interface inspection are possible, and 100 GHz images identify interfacial water using the pulsed THz system.
- In particular, an inexpensive 200 GHz source could be implemented in the TeraSense scanning prototype to optimize sensitivity to interfacial water layers for further study.

- Further work with the microwave scanning to determine if sensitivity to interfacial water can be observed would allow a COTS for the application via Spectrum NDT.

4.3 – Conclusion. We conclude that the proof-of-principle was successful to demonstrate concealed interface imaging using frequencies ranging from microwave to 0.3 THz. Furthermore, interfacial water can be detected with the THz system, and potentially with the microwave system as well.

Appendix 1 – Spectrum NDT report (subsequent pages)

SpectrumNDT Non-Metallics

Microwave Interferometry Inspection Report of Semi-Transparent Sample

UNBC/DRDC

Jordan Hynes

Spectrum NDT

March 2017

Spectrum NDT Non-Metallics

Introduction

Spectrum NDT was asked to perform microwave interferometry inspection on a semi-transparent sample through the University of Northern British Columbia. The work was done at CFB Esquimalt for DRDC. This was the second round testing, as the first semi-transparent samples carbon content was too high for the microwave energy to pass through. The semi-transparent sample in this trial has a presumably lower carbon content, and was placed on top of a steel backing plate with machined defects.

Inspection

The microwave equipment that was used is a first-gen portable hand scanner. It uses a infrared camera and a tacker on the probe to follow the location of the probe and map the distance traveled. Being that is the operator must physically move to probe back and forth there can be nonrelevant indications from probe wobble on the images.

2 probe frequencies were used, a 10mhz and a 24mhz, with the 24mhz providing the best scan images.

The first test was to place a small piece of aluminum foil tape on the underside of the semi-transparent sample and perform a scan to ensure that the microwaves are penetrating though the sample. First test with the 10mhz, fig1.

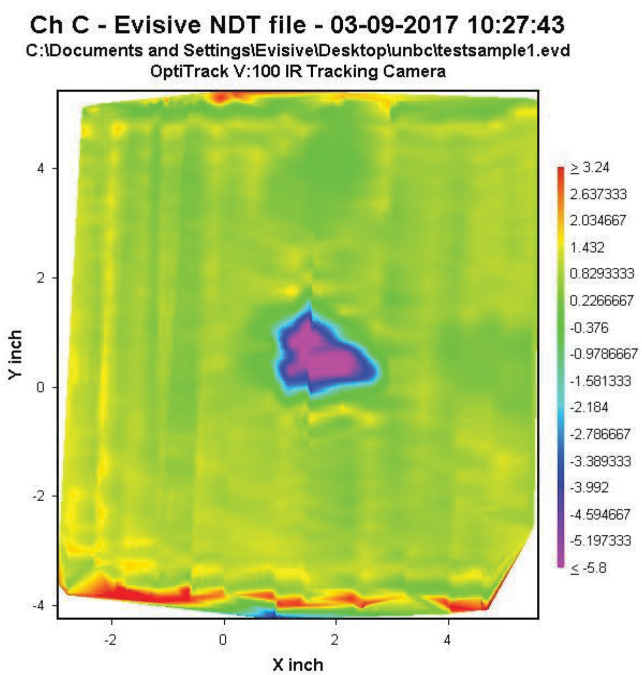

Figure 1

Next was to test the 24mhz, the results were better than the 10mhz. The L shape of the foil is better defined and the 2 diagonal white lines (yellow arrows) are from the folded seams of a cardboard box that was under the sample and a ½” plastic sheet. All of the vertical lines are from the movement of the hand scanner and consistent on all the images. After comparing the 10mhz to the 24mhz it was determined that the 24mhz would be used for the rest of the testing due to the higher resolution.

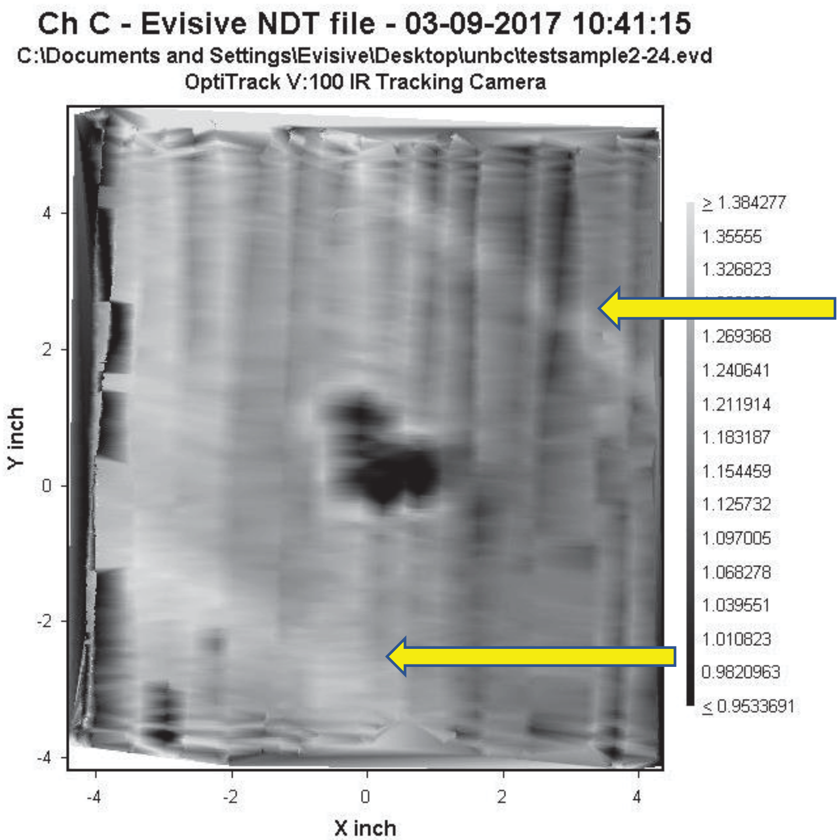

Figure 2

The next tests were done on the steel plate that had various sized machined out holes and channels, fig 3.

Figure 3

Scan 3 was done over top of the large area with the recessed circle in the middle, along with the thin machined strip (fig4.).

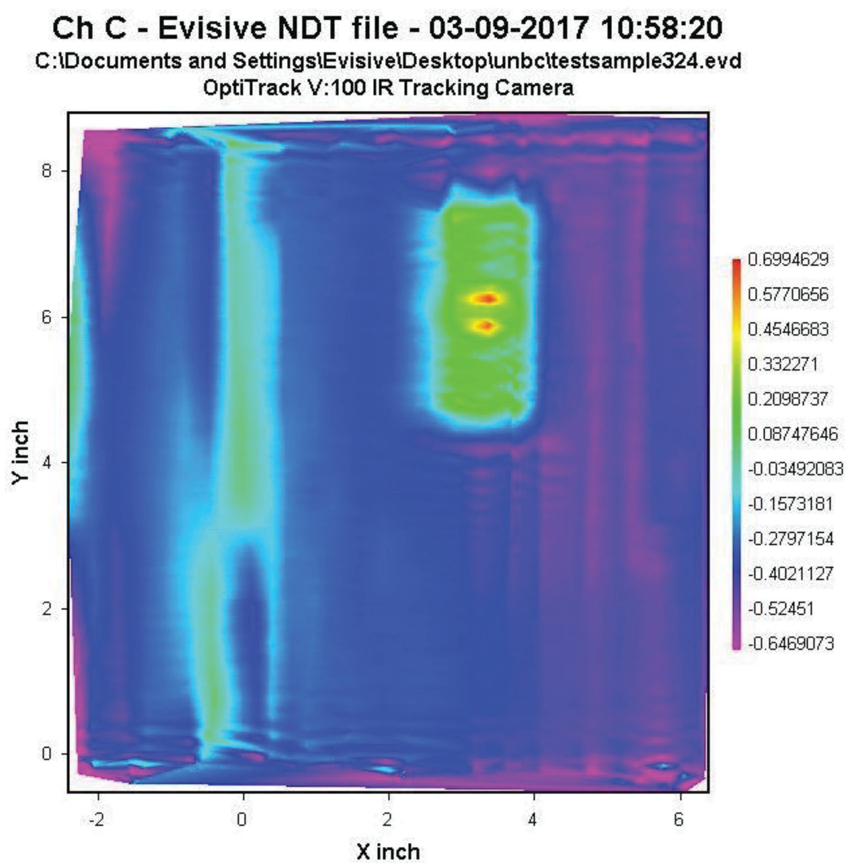

Figure 4

In scan 5 there was a thin plastic sheet placed under with a small square hole cut out of it, it was placed at the top of the scan area. Even though the square hole wasn't found there is difference where the plastic was placed. The black area is where the plastic is, and the red area is the semi-transparent sample touching the metal, fig 5. The 2 spots on the bottom right are nonrelevant indications (black arrow).

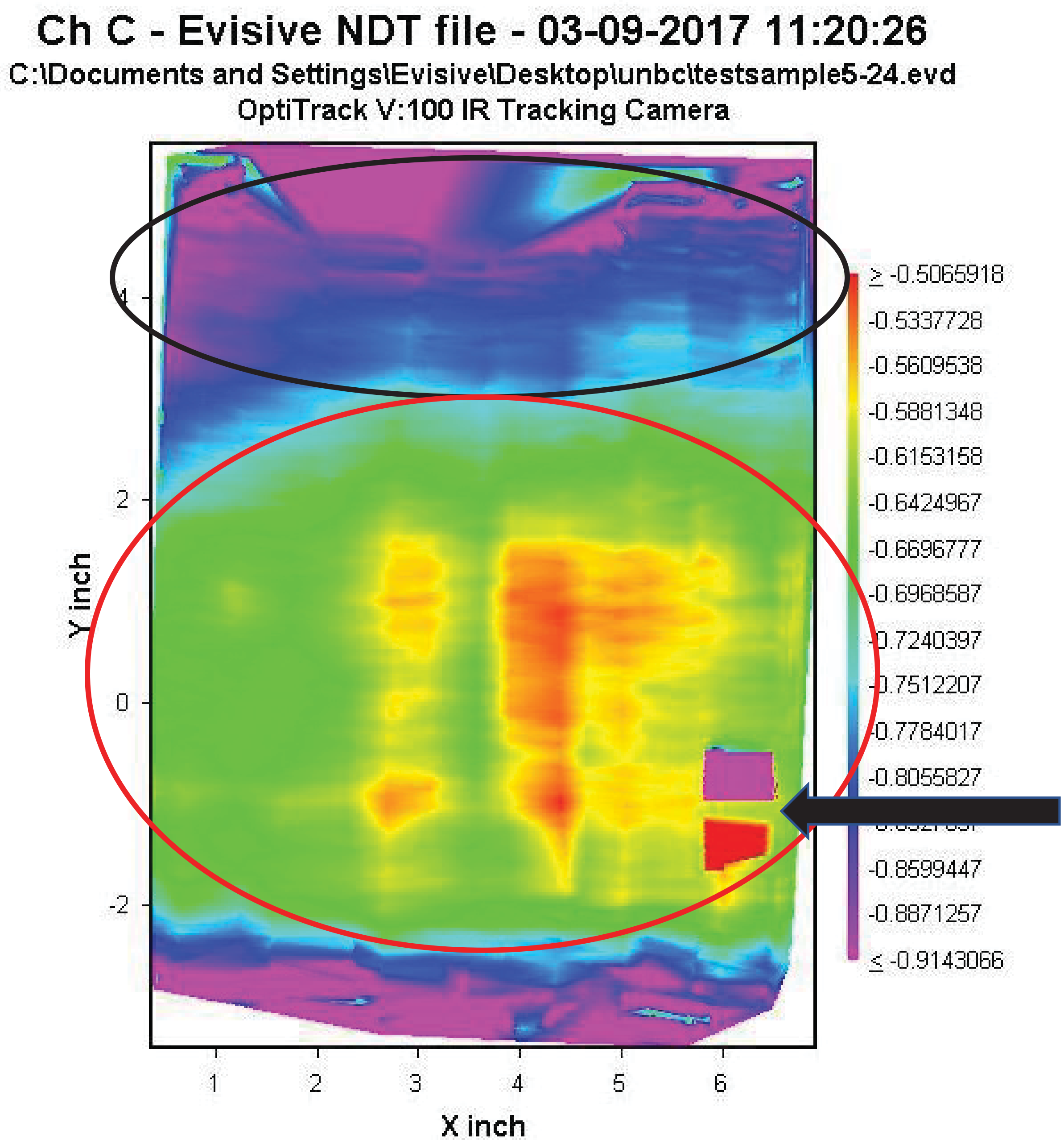

Figure 5

In scan 6 the smaller hole (yellow arrow) was filled with water, but once the semi-transparent sample was lifted off the water had wicked out and was spread all over, fig 6.

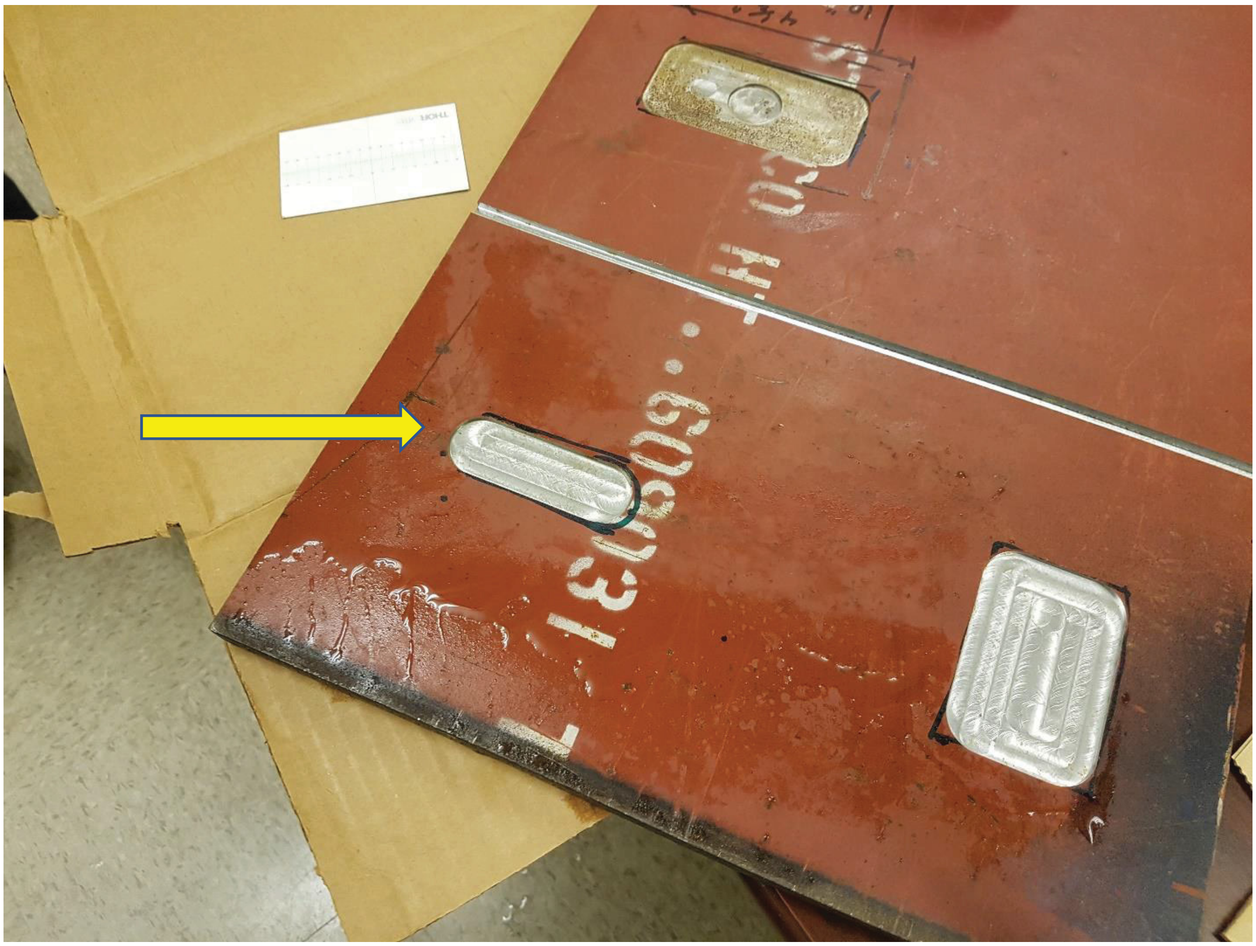

Figure 6

When looking at the scan image, this area that has the water between the sample and plate does show up as slightly more reflective, (black rectangle) fig 7. The area to the right of the thin channel appears to be a small air gap and could have been the sample not sitting completely flush on the plate (red oval).

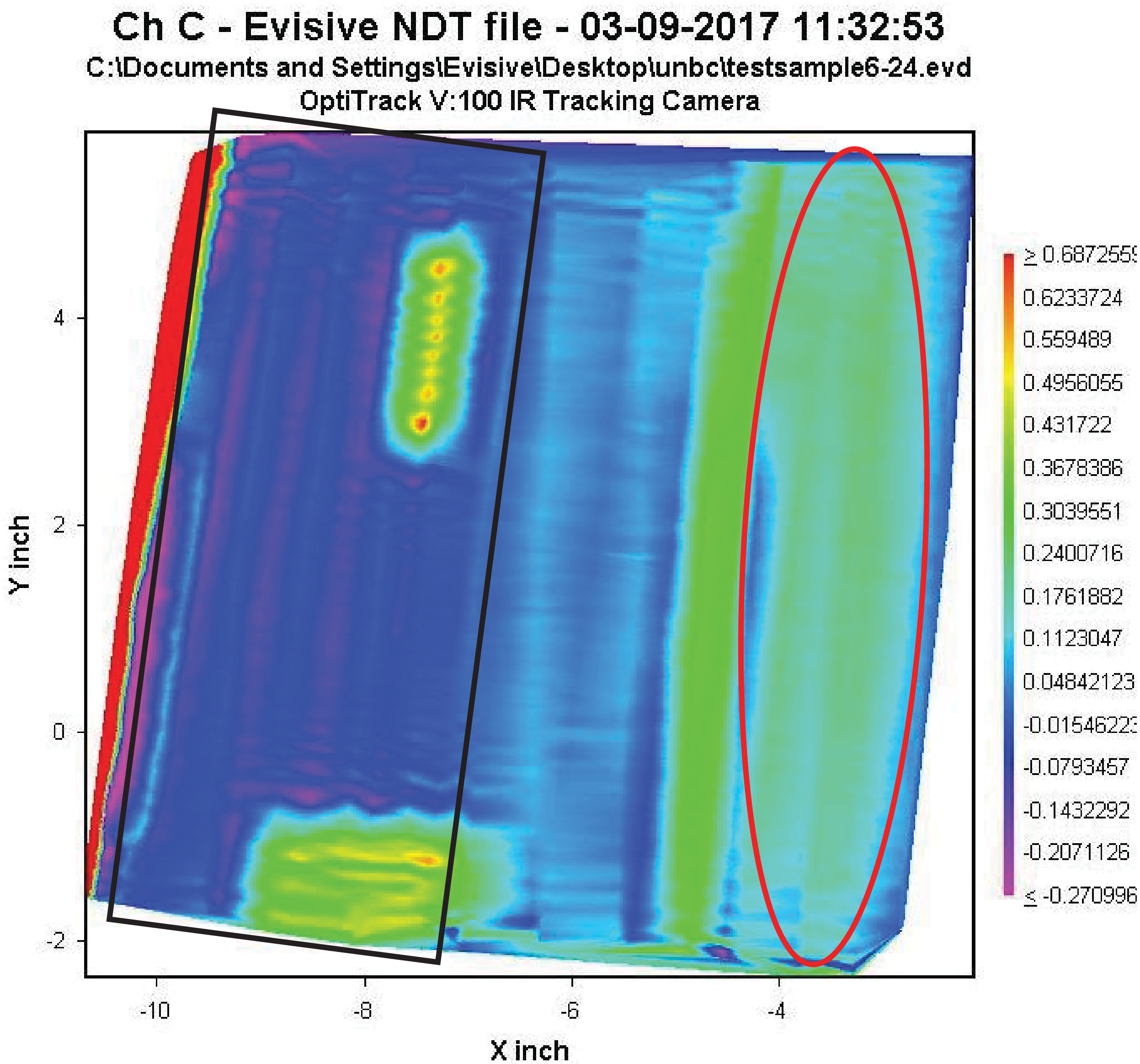

Figure 7

For scan 7, water as placed into the thin channel and in the round hole inside the large rectangular hole, see fig 8 for before. In fig 9 is how the water had moved out of the channel after the semi-transparent sample was removed.

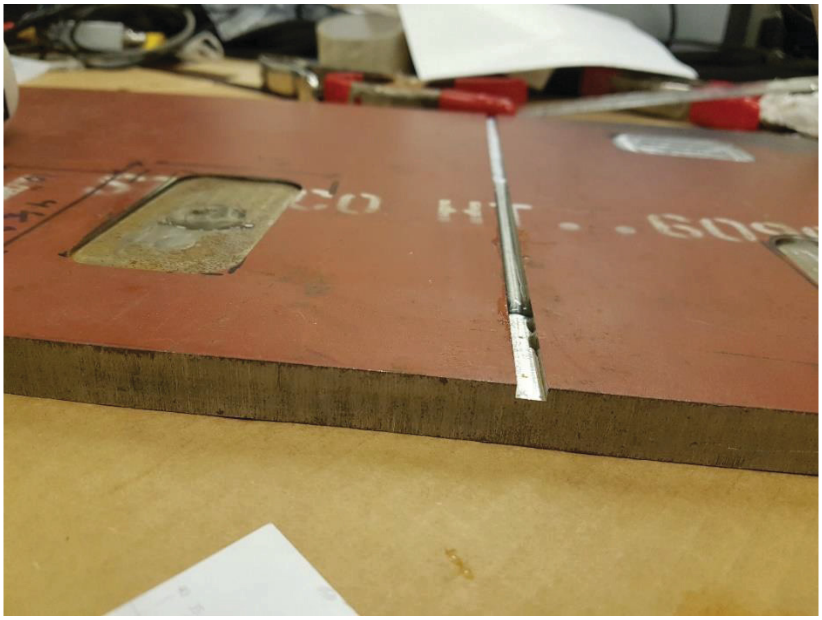

Figure 8

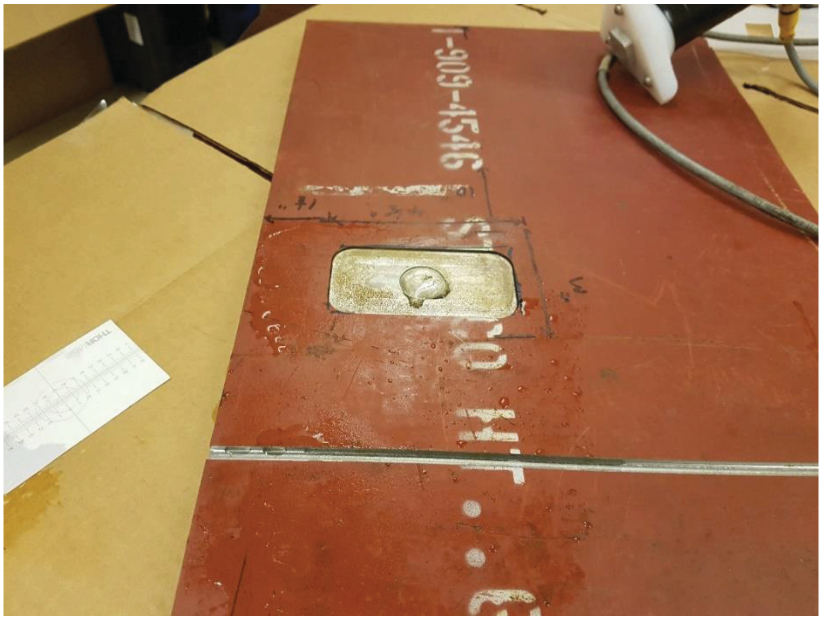

Figure 9

Similar to scan 6, the water that has wicked out of the channel is showing an overall voltage change (black rectangle). The water inside the small circle (red circle) is also providing a notable change in voltage. It is unclear at this time if it is only because the air gap in that area is now no longer there, or the actual presence of the water. Once the semi-transparent sample was removed there was a small wet spot on the underside that lined up with the small circle area, fig10.

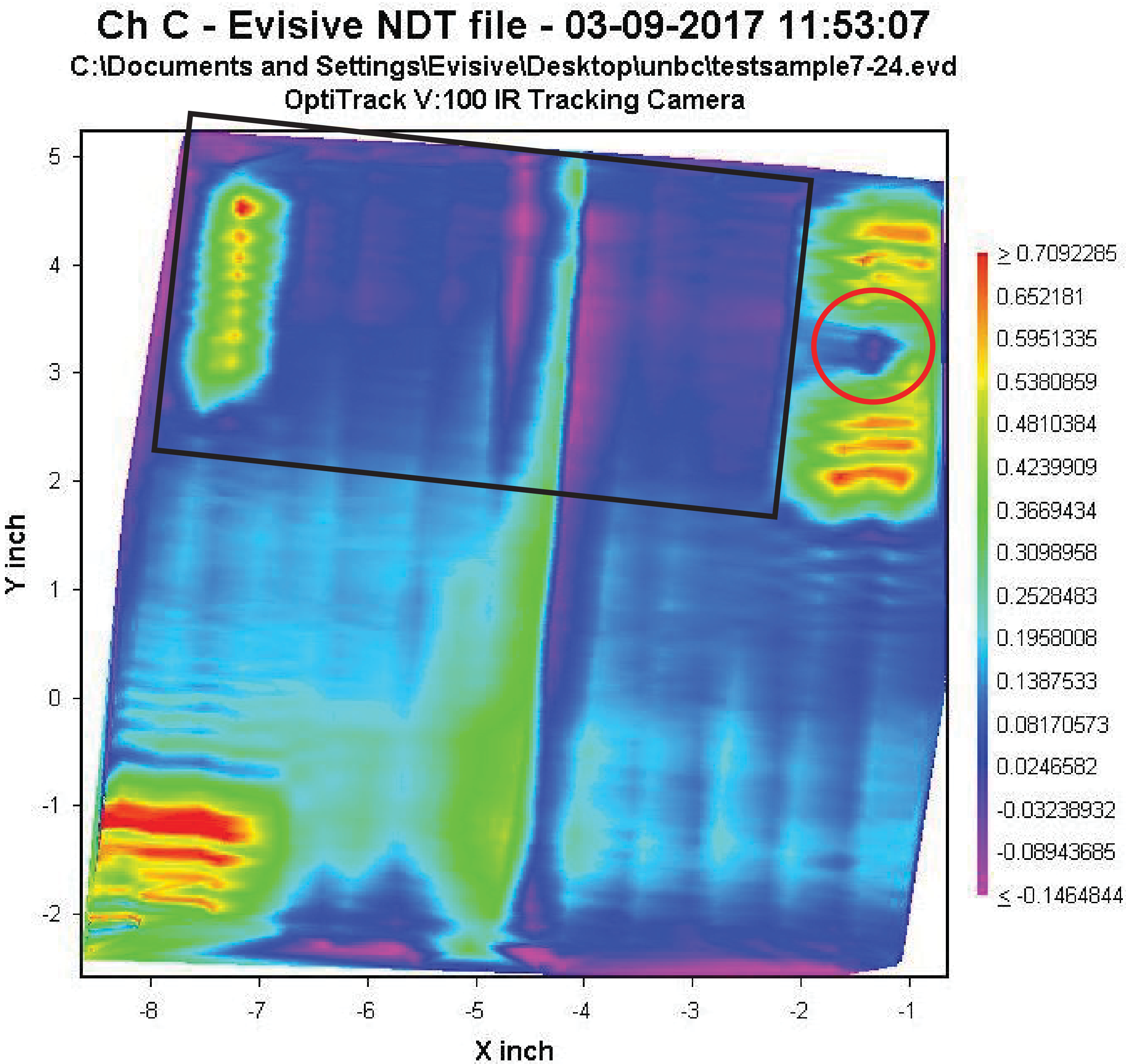

Figure 10

In Scan 8 (fig 11) the small circle area inside the larger rectangular hole was filled with water and the semi-transparent sample placed in the same position as scan 3 (fig 12) so there would be a comparison between with and without water. It is very clear that the water is there.

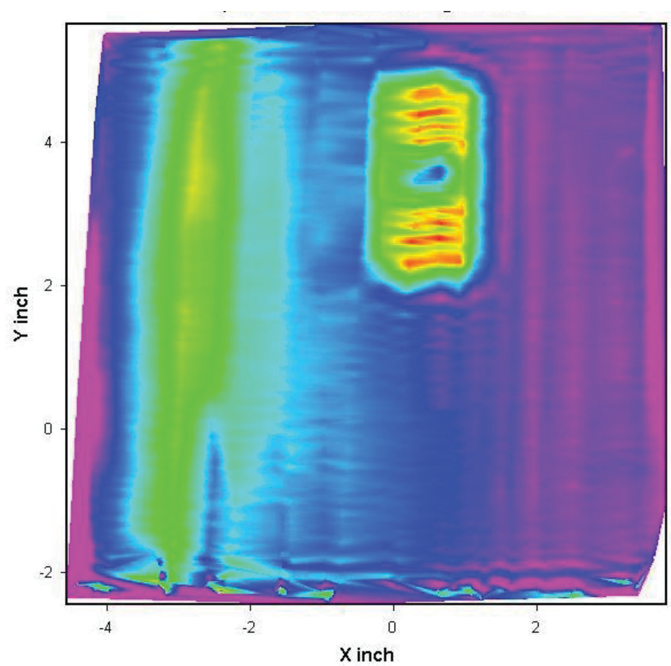

Figure 11 Water

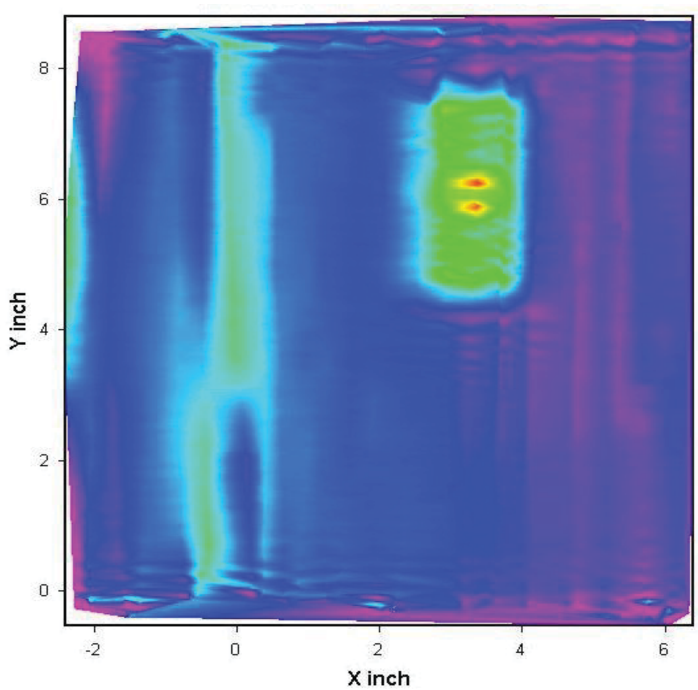

Figure 12 No Water

In scan 9 there was a small drop of water placed in a bare spot on the steel plate, Fig 13 is the before picture and Fig 14 is after the sample was removed.

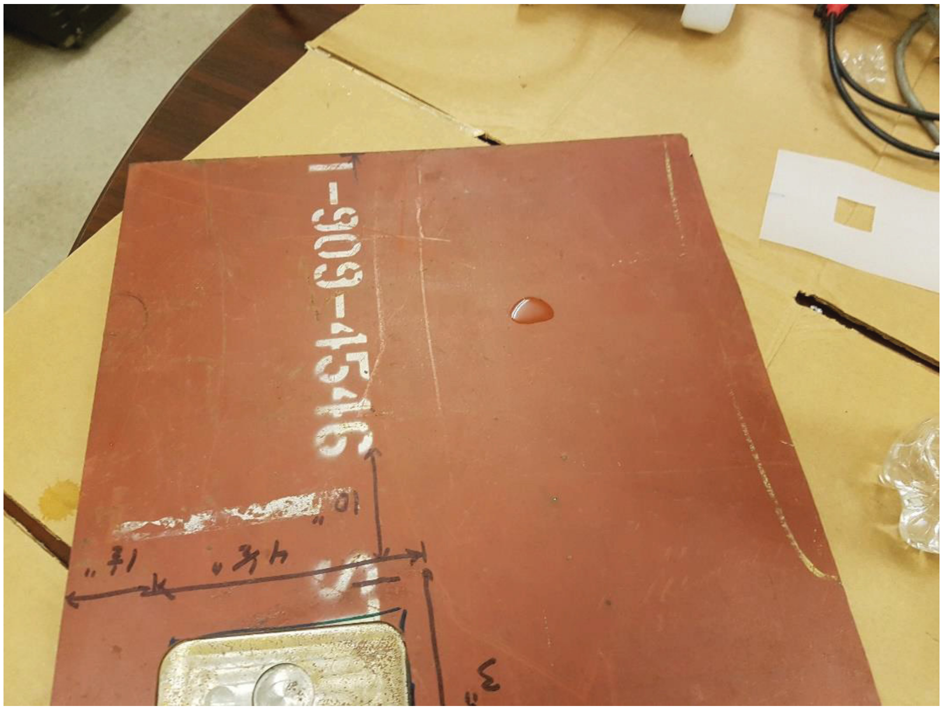

Figure 13

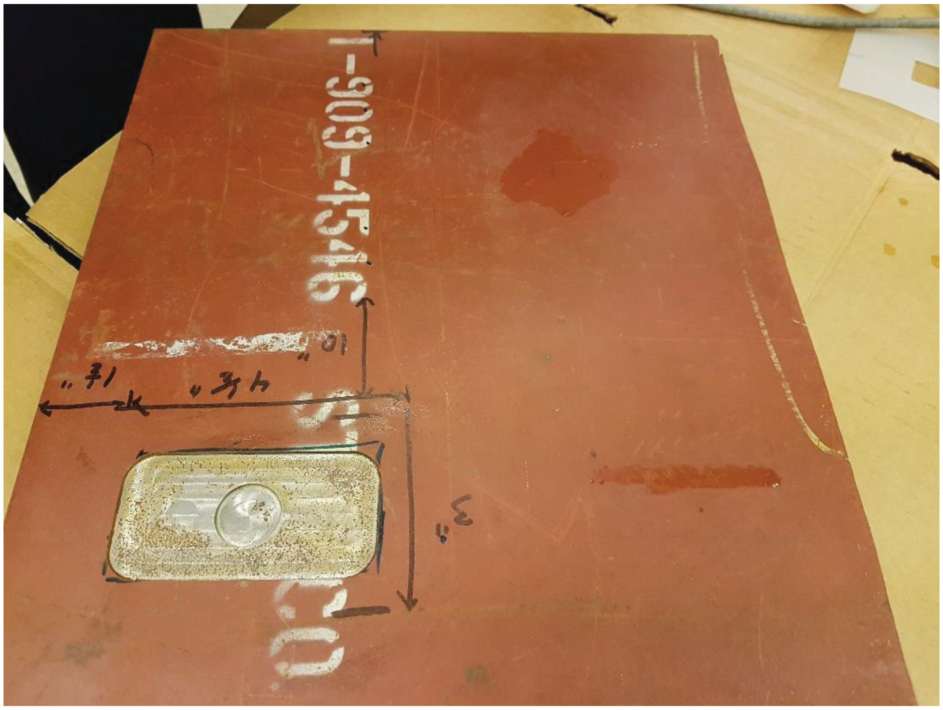

Figure 14

In the scan image (fig 15), there is no visible indication of the water. The location of the water droplet was at XY(3,1).

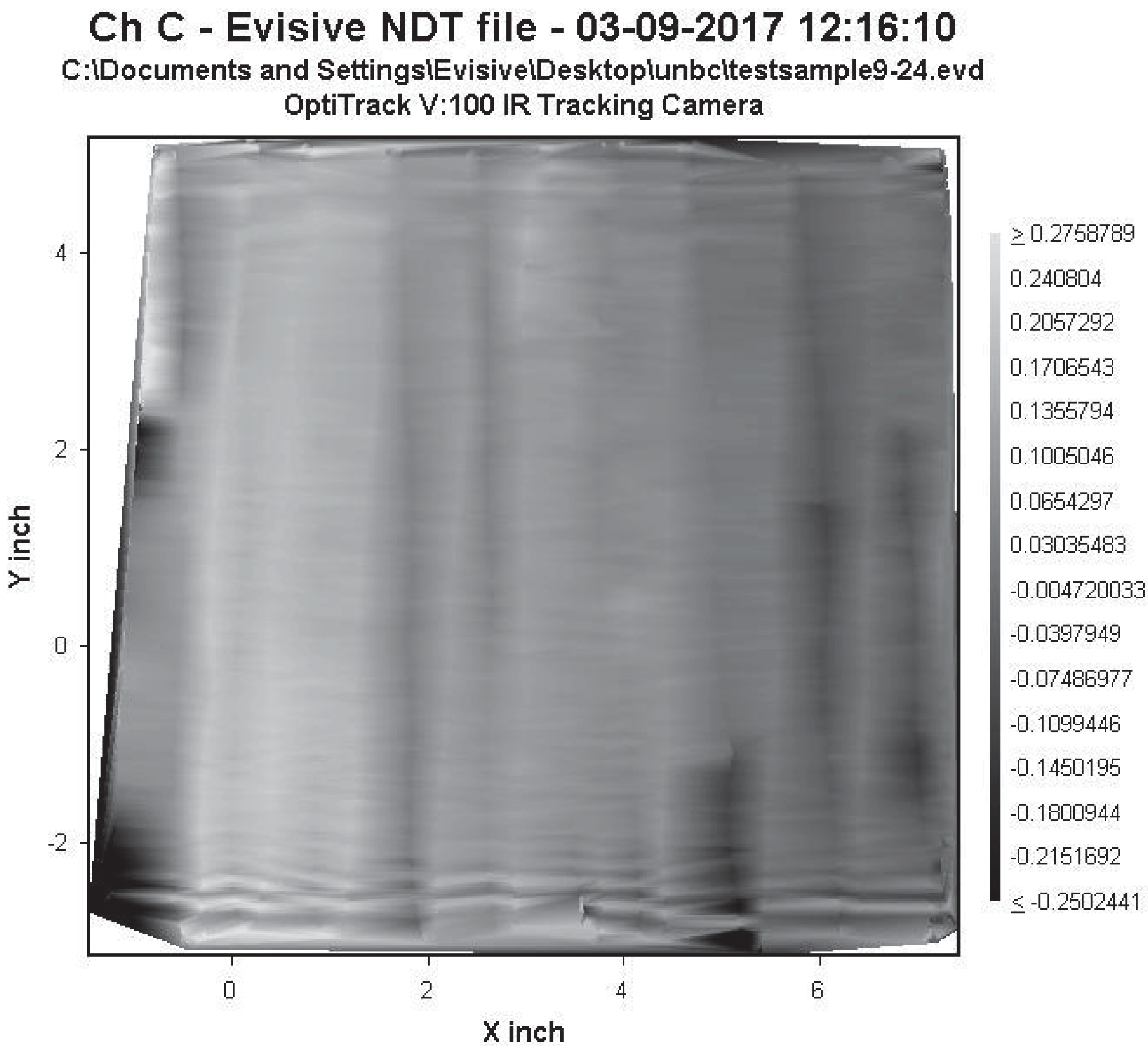

Figure 15

Conclusions

There are several conclusions from the minimal amount of testing that was performed:

- The machined areas (i.e. larger air gaps) were quite easy to locate, and their varying depths have an influence on signal return
- The presence of water can alter the signal return notably
- The semi-transparent sample (as inspected) is transparent to microwave energy at 10 – 25GHz

The water is reflecting a signal to a certain extent, however it is unknown how much water is required to create the signal difference. As well, it is unknown whether the water is creating the signal change, or if the water is indeed creating a changing air gap between the panel and the steel backing.

Based on the results of the experiment it can be concluded that microwave energy can be used to see through a dielectric material and differentiate properties of the interface and conductive backing material.

DOCUMENT CONTROL DATA

*Security markings for the title, authors, abstract and keywords must be entered when the document is sensitive

1. ORIGINATOR (Name and address of the organization preparing the document. A DRDC Centre sponsoring a contractor's report, or tasking agency, is entered in Section 8.) University of Northern BC 3333 University Way, Prince George (BC) V2N 4Z9 Canada	2a. SECURITY MARKING (Overall security marking of the document including special supplemental markings if applicable.) CAN UNCLASSIFIED 2b. CONTROLLED GOODS NON-CONTROLLED GOODS DMC A

3. TITLE (The document title and sub-title as indicated on the title page.)

Exploring Terahertz Waves for Submarine Cladding Non-Destructive Examination (NDE): Tile Sealant Transmission Characterization, Instrument Field Housing Design/Prototype Option B: proof-of-concept concealed interface imaging

4. AUTHORS (Last name, followed by initials – ranks, titles, etc., not to be used)

Reid, M.; Kilcullen, P.

5. DATE OF PUBLICATION (Month and year of publication of document.)	6a. NO. OF PAGES (Total pages, including Annexes, excluding DCD, covering and verso pages.)	6b. NO. OF REFS (Total references cited.)
March 2017	32	0

7. DOCUMENT CATEGORY (e.g., Scientific Report, Contract Report, Scientific Letter.)

Contract Report

8. SPONSORING CENTRE (The name and address of the department project office or laboratory sponsoring the research and development.)

DRDC – Atlantic Research Centre
Defence Research and Development Canada
9 Grove Street
P.O. Box 1012
Dartmouth, Nova Scotia B2Y 3Z7
Canada

9a. PROJECT OR GRANT NO. (If appropriate, the applicable research and development project or grant number under which the document was written. Please specify whether project or grant.)	9b. CONTRACT NO. (If appropriate, the applicable number under which the document was written.)
01eb - RCN - Ships Systems Readiness	W7707-155881/001/HAL
10a. DRDC PUBLICATION NUMBER (The official document number by which the document is identified by the originating activity. This number must be unique to this document.)	10b. OTHER DOCUMENT NO(s). (Any other numbers which may be assigned this document either by the originator or by the sponsor.)
DRDC-RDDC-2018-C200	Client Ref. No.: W7707-16-5881

11a. FUTURE DISTRIBUTION WITHIN CANADA (Approval for further dissemination of the document. Security classification must also be considered.)

Public release

11b. FUTURE DISTRIBUTION OUTSIDE CANADA (Approval for further dissemination of the document. Security classification must also be considered.)

12. KEYWORDS, DESCRIPTORS or IDENTIFIERS (Use semi-colon as a delimiter.)

Non-destructive testing/inspection; Submarine; Acoustic tile; Water detection

13. ABSTRACT/RÉSUMÉ (When available in the document, the French version of the abstract must be included here.)

A Brewster angle imaging system was developed for subsurface hull inspection using broad-band pulsed THz radiation using a Picometrix T-Ray 4000 system in a previous phase of this project. Additionally, a single frequency, reflection imaging prototype system was developed using a cw TeraSense sub-THz imaging camera for subsurface interface inspection. Both systems were previously used to look at the possibility of a submarine hull inspection application for water ingress below Sikaflex grout lines, as it was identified that the grout-lines held the only potential for thoughcladding hull inspection in the far-infrared. Additionally, the possibility of using microwave frequencies was studied by subcontracting microwave inspection to Spectrum NDT. It was identified that through-Sikaflex inspection was not possible at frequencies of potential transparency at frequencies in the far-infrared and below (below 2 THz). In order to generally explore the suitability for subsurface interface water ingress detection of the developed prototypes at all frequencies, the project was extended as per Option B, to demonstrate the potential of the envisioned systems to tackle the identified problem using an analogue sample as the cladding, to demonstrate the idea. As such, this report summarizes the potential for the envisioned application in the far infrared using (i) the pulsed THz Brewster angle imaging system developed in the previous phase, (ii) the cw TeraSense reflection imaging system prototype developed in the previous phase, and (iii) the evisive scan microwave system subcontracted in the previous phase of this project. The results demonstrate the proof-of-principle of concealed interface inspection is possible, and we offer insight into subsurface interface inspection and moisture detection at frequencies from microwave to THz. DRDC Technical Authority Note Regarding Significance for Defence and Security : This report demonstrates the ability of THz waves and this developed equipment, to conveniently and non-destructively detect sea water contamination beneath homogeneous (i.e. no internal void) designs of thick dielectric acoustic coating on submarines.